Disulfide bonds: the power switches of elastic proteins

Edward C. Eckels[#,1,2], Shubhasis Haldar[#,1], Rafael Tapia-Rojo[1], Jaime Andres Rivas Pardo[1], Julio M. Fernández[1]

[#] These authors contributed equally to the work
[1] Department of Biological Sciences, Columbia University, New York NY 10027
[2] Integrated Program in Cellular, Molecular, and Biomedical Studies, Columbia University Medical Center, New York NY 10032

The delivery of mechanical power, a crucial component of animal motion, is constrained by the universal compromise between force and velocity of its constituent molecular systems[1,2]. Here we demonstrate a switchable power amplifier in the elastic proteins that comprise contractile tissues. Elastic proteins are typically very large and composed of tandem repeats of individually folded domains[3–5], which unfold and extend under force and readily refold when the force is quenched. Cryptic cysteine residues are common in elastic proteins like titin where they can oxidize to form intra-domain disulfide bonds, limiting the extensibility of an unfolding domain[6–8]. However, the functional significance of disulfide-bonds in elastic proteins remains unknown and may be fundamental to tissue mechanics. Here we use ultra-stable magnetic tweezers force spectroscopy[9,10] to study the elasticity of a disulfide bonded modular titin protein operating in the physiological range, with the ability to control the oxidation state of the protein in real time. We show that the midpoint folding probability of the parent Ig domain reversibly shifts from 4.0 pN to 12.8 pN upon oxidation. In this force range, the folding contraction dominates the elastic recoil of the protein, delivering stepwise mechanical work which depends on the oxidation state in an all-or-none manner. For example, the output power of a folding contraction at 6 pN goes from 0 zW to 6,000 zW upon introduction of the disulfide bond. This large amount of power is delivered by folding at forces where single molecular motors are typically stalled. We explain our results with a simple polymer model where the extensibility of the protein is determined in a binary form by the presence or absence of the disulfide bond. Our results demonstrate, for the first time, the functional significance of disulfide bonds as potent power amplifiers in proteins operating under force.

Mechanical systems are defined by their force-velocity relationship, which measures the magnitude of the work they perform and the rate at which they deliver it. This physics holds true on scales ranging from man-made machines down to single molecule actuators and determines the peak power that can be delivered by a mechanical system[1]. In biological organisms, the magnitude of the mechanical power delivered determines the timescales on which it can respond to its environment, for example to evade a predator or to capture a prey. For these reasons, evolution has driven biological systems to optimize their power delivery. We know of many molecular scale actuators such as motors[11–13], filament torsion[14,15], assembly[16,17] and disassembly[18] that can deliver surprisingly large amounts of mechanical power on the scale of about ~1000 zW per molecule. Mechanical power scales in networks of these molecules, reaching levels that are compatible with the environment of the organism[2]. Thus, delivery of mechanical power is a central issue in understanding biological design, but very little is known about what dictates the mechanics at a molecular level in these power delivery systems. One important addition was the discovery that protein folding does a large amount of mechanical work, on par with that measured in other molecular systems[9,19]. However, the force-velocity relationship for protein folding has never been measured and the power capabilities of a folding-driven molecular actuator remain unknown. Titin, the giant elastic protein of muscle tissues is a likely candidate for being an important source of mechanical power derived from folding[20]. A unique characteristic of titin is that the majority of the tandem Ig domains of its elastic region are disulfide bonded, yet the role of disulfide bonds in power delivery is unknown[6,7]. Here we use

ultra-fast single molecule magnetic tweezers to determine the force-velocity relationship of folding from a short, disulfide-bonded titin segment, and demonstrate that oxidation of a single disulfide bond in the core of the protein boosts the power delivery from folding in an all-or-none manner thus acting as a power switch.

The magnetic tweezers instrument provides a natural way for probing the force-velocity relationship of a nanomechanical system because it supplies a constant-force field along with high resolution tracking of folding trajectories. Here we measure the force-velocity relationship of a tandem modular protein construct containing eight repeats of cardiac titin Ig domain I27 with two cysteines that can form a single disulfide bond. The eight identical repeats of the I27 domain in the expressed construct generate an unambiguous fingerprint upon unfolding. In the oxidized form ($I27^{OXD}$), the formed disulfide limits the extension of the amino acid backbone upon unfolding (Figure 1A), resulting in 11 nm upwards steps as each Ig domain unfolds up to its disulfide bond (Figure 1B, blue trace) during the *extend* pulse. In contrast, the same Ig domains with the reduced disulfide ($I27^{RED}$) demonstrate 25 nm upwards steps, identical to those observed in the wild-type I27 domain (Figure 1B, red trace). After unfolding, the force is reduced to allow the polypeptide backbone to collapse during the *refold* pulse. There is a marked difference in the folding trajectories of the reduced and oxidized Ig domains – the reduced Ig domains demonstrate a gradual downward stepwise trajectory, a combination of six downward events and two upwards events, indicating a net total of four folding events. By pulling again at high force in the *probe* pulse, the four 25 nm unfolding steps confirm the refoldng count. By contrast, the oxidized Ig domain shows immediate collapse during the refolding pulse and eight 11 nm steps during the probe pulse, demonstrating complete refolding.

The oxidation status of the disulfide bond can be controlled in real-time as depicted in the chart-recorder style single molecule trace in Figure 1C. In this experiment, the molecule is first stretched at high force (84 pN) to unfold eight oxidized Ig domains, each with a step size of 11 nm (inset histogram, Fig. 1C). The force is quenched to 2.8 pN to allow for refolding while a buffer containing 10 mM tris(2-carboxyethyl) phosphine (TCEP) is prepared for exchange into the chamber. Unfolding the molecule again at high force demonstrates eight upwards steps of 11 nm, after which the reducing buffer is introduced through three successive washes of 100 uL, a volume ten-fold higher than the volume contained inside the flow cell. Reduction by TCEP leads to eight successive 14 nm steps caused by cleavage of the disulfide bond and release of the cryptic length sequestered behind the bond (Figure 1A). With the reducing agent still present in the solution, the force on the molecule is again quenched to 2.8 pN to allow for refolding. A final probe pulse at 84 pN demonstrates eight 25 nm steps – indicating complete refolding of the protein in its reduced state.

This assay was used to determine the folding probability of the oxidized versus reduced Ig domain over a wide range of forces. After unfolding the $I27^{OXD}$ construct using an *extend* pulse, the refolding force was clamped at a force ranging from 5-18 pN for 100 s, after which the *probe* pulse revealed how many domains had folded (Figure 2A). The $I27^{OXD}$ domains experienced very little refolding at 15.3 pN, occasionally one domain per octamer, but exhibit 7 folding events at a refolding force of 10.6 pN. The step sizes observed during the refolding pulse scale

according to the freely-jointed chain (FJC) polymer model[21] and match the previously reported value for contour length[22], 12.7 nm, with a slightly larger Kuhn length of 0.70 nm that is a better fit in the low force regime explored by the magnetic tweezers (Figure 2C). After obtaining the data from the oxidized domain, the protein was reduced with 10 mM TCEP, which was kept in solution to prevent spontaneous re-oxidation or unwanted side reactions of the two reduced cysteine residues while measuring the folding probability. The $I27^{RED}$ construct showed dramatically different folding trajectories, requiring forces as low as 5 pN to begin refolding, and forces down to 2.5 pN for complete refolding of all eight domains (Figure 2B). These size of refolding events also demonstrated scaling with the FJC model, with a Kuhn length of 1.27 nm, and a contour length of 28.4 nm (Figure 1C, red curve). The folding probability as a function of force demonstrates a large, 8.4 pN shift in the midpoint of the folding probability according to the fit with a sigmoid curve (Supplementary Methods). This shift is clearly demonstrated by the data, which shows rapid refolding of the $I27^{OXD}$ domains at a force of 10.6 pN, but rather slow refolding from $I27^{RED}$ at a force of 4.3 pN. The cause of this increase in the folding kinetics and lowering of the refolding barrier may arise from either the reduced entropy of the backbone imposed by the presence of the disulfide bond or perhaps some residual structure in the peptide loop delimited by the disulfide bond that serves to nucleate folding.

From these measurements, it is not immediately clear if presence of an extension-limiting disulfide bond will increase or decrease the mechanical work delivered by a folding Ig domain because higher folding forces and smaller step sizes have opposite effects on work delivery. The maximum work can be calculated simply as the product of the applied load and the mean step size at that force. However in the force range explored for titin folding, there is an equilibrium between folding and unfolding steps, so the net amount of work delivered by folding a single titin Ig domain is equal to the maximum work (empty squares, Figure 3) times the folding probability (empty diamonds, Figure 3). This quantity is called $< W >$, the expected value of the work output[9] (solid circles, Figure 3). The $I27^{RED}$ folding process generates a peak $< W >$ of only 25.6 zJ at 4.2 pN whereas $I27^{OXD}$ folding work peaks at a value of 63.9 zJ and 11.7 pN (Figure 3, solid curve). Oxidation of the single disulfide bond in this protein therefore doubles the magnitude of the expected work performed Ig domain folding. Although these work values are on the same order of magnitude as other molecular actuators, a better assessment of the relevance of protein folding on a physiological scale is the rate at which the energy is delivered.

During a muscle contraction, force development occurs within milliseconds after activation of the muscle fiber[23], redistributing some of the load from titin to the crossbridges themselves. Here we aim to mimic these force changes in titin using ultra-fast force quenches to determine if there is significant power output from titin on the relevant timescales (Figure 4A). After a high force *extend* pulse at 80 pN, the force was ramped down to 16 pN over the course of 0.5 seconds, where $I27^{OXD}$ does not fold (Figure 2C). After settling at 16 pN for 1 second, the magnets were stepped as quickly as possible (~5 ms) to provide a force in the range of 2-10 pN. Tracking of the protein trajectory after these very fast force quenches permits a measurement of the power output due to protein folding. As seen in Figure 4A, the folding trajectories are so rapid that it is difficult to distinguish individual folding steps. The change in length at 16 pN before and after

the force quench, as well as the presence of eight steps in the final probe pulse (not shown), indicate complete refolding of the protein construct. The force ranges over which the folding kinetics could be tracked were 3-10 pN for $I27^{OXD}$ or 2-3 pN for $I27^{RED}$. The lag introduced by changing the magnet position and the amplitude of the folding contraction were the limiting factors at lower forces. The effective shortening rate during the refolding pulse was determined by fitting a single exponential to the trajectory (inset, Figure 4A). The amplitude of the exponential was fixed to eight times the step size as predicted by the freely-jointed chain model (Figure 2D), thereby excluding the entropic collapse of the polymer due to the change in force. The observed rate constants are plotted for both the oxidized and reduced forms of the protein are shown in Figure 4B, blue and red data points, respectively. The folding rates are fit with a modified exponential model that takes into account the free energy of a polypeptide[24,25] modeled as a freely-jointed chain polymer extended up to the pulling force:

$$k_{FJC}(f) = k_0\, exp\left[-\frac{\Delta L_C}{l_K}\left(ln\left|sinh\left(\frac{F\cdot l_k}{k_B T}\right)\right| - ln\left(\frac{F\cdot l_k}{k_B T}\right)\right)\right] \quad (1)$$

Here ΔL_C is the contour length and l_k is the Kuhn length as determined from the previous fits to the freely jointed chain. The curvature of the folding rates due to movement of the folding transition state with force is well accounted for by this model (dashed fits, Figure 7B). In a mechanics experiment used to determine the force-velocity relationship of muscle, shortening velocities are recorded after a small step change in the load. The muscle fiber typically exhibits <100 nm shortening per half sarcomere over tens of milliseconds[26–28]. Therefore we consider the initial shortening velocity, v_0, of a titin molecule as the physiologically relevant measurable here. The velocity, v_0, is the slope of the folding trajectory at time zero and is calculated from the amplitude of the exponential fit multiplied by the force dependent folding rate, given by

$$v_0 = N\cdot x_{FJC}\cdot k_0\, exp\left[-\frac{\Delta L_C}{l_K}\left(ln\left|sinh\left(\frac{F\cdot l_k}{k_B T}\right)\right| - ln\left(\frac{F\cdot l_k}{k_B T}\right)\right)\right] \quad (2)$$

where N is the number of folding domains and x_{FJC} is the force dependent step size of folding calculated from the freely jointed chain. Unlike the force-velocity relationship of muscle, which does not have a maximum according to the hyperbolic Hill equation, the force-velocity relationship shown here is peaked due to the rapidly diminishing folding step size as the force approaches zero. Despite the contour length of the $I27^{OXD}$ being less than half that of the reduced domain, the incredibly accelerated folding rate causes the folding velocity of $I27^{OXD}$ to be ~300-fold higher at a force of 3 pN. From these data, the power output can be easily calculated by multiplying the applied force by the measured shortening velocity.

$$P_0 = F\cdot N\cdot x_{FJC}\cdot k_0\, exp\left[-\frac{\Delta L_C}{l_K}\left(ln\left|sinh\left(\frac{F\cdot l_k}{k_B T}\right)\right| - ln\left(\frac{F\cdot l_k}{k_B T}\right)\right)\right] \quad (3)$$

The power output of this disulfide bonded titin construct reaches much higher than any other protein ever observed, up to 5,870 zW measured at a pulling force of 4 pN, with a predicted

peak power of 6,530 zW at a force of 3.6 pN according to the fit by equation (3). By contrast, the largest power output measured from the reduced domains reaches only to 21 zW at a force of 2.5 pN. This is comparable to, but slightly under the power output estimated from the wild type I27 and I10 domains (neither contain a disulfide bond), which reach approximately 200 zW. From these measurements it is clear that the disulfide bond acts as a switch that doubles the amount of work done by folding, but is able to boost the power output of folding by several orders of magnitude.

Cysteine chemistry plays a very broad yet poorly understood role in regulation of cytoskeletal mechanics, and there is no elastic tissue where cysteines are more highly concentrated than in muscle. The dense packing of proteins in the sarcomere creates an environment where the local concentration of protein thiols reaches into the millimolar range, and is thus competing with antioxidant thiols for modification by reactive oxygen species. In muscle tissue, oxidation of cysteines of the ryanodine receptor alters calcium release dynamics[29–31], and ROS mediated S-glutathionylation of protein thiols in myosin, titin, myosin binding protein C, troponin, and actin have all been demonstrated to alter muscle mechanics and calcium sensitivity[32]. Here we have demonstrated that disulfide bonding is a switch-like regulator of the power output from Ig domain folding, converting a soft and extensible polypeptide into a potent power-delivery device. At a force of 6 pN, the reduced protein domain is completely unable to fold (Figure 2B). Simple oxidation of the disulfide bond allows the protein to fold at the same force of 6 pN with a predicted step size of 4 nm, each step thus delivering 24 zJ of work. With an initial folding velocity of 1,000 nm/s, this equates to a power delivery of 6,000 zW. The switch like behavior reported here is easily tuned by the redox status of the muscle, which changes with exercise, stress, and ischemia. Most importantly, oxidation of the disulfide bond aligns the folding forces and velocities with those observed in myosin II motors. Single molecule optical tweezers experiments show that single myosin II power strokes generate steps of 12 nm and forces of 3.4 pN on average[13]. Other studies using ensembles of myosins to enable continuous sliding against a pulling force report velocities of 500 nm/s at forces of 3 pN per motor[33]. Harnessing the chemical potential energy of ATP is only one means by which animals power their motion; storage of gravitational potential energy and inertia in elastic proteins such as the Ig domains studied here creates a hybrid mechanical system that can be tapped to deliver explosive levels of power through the synergy of protein folding and mechanochemical cycling of the myosin. It is therefore highly likely that the unique material properties of elastic proteins, which we have demonstrated here, are used to power motion in heretofore undiscovered molecular and cellular systems.

Methods Summary

Instrumentation and protein purification: All single molecule magnetic tweezers experiments were performed as described previously, utilizing HaloTag chemistry for attachment to the glass and biotin-streptavidin for attachment to superparamagnetic beads[9,10]. The octameric I27 DNA constructs were assembled as described previously[8]. $I27^{OXD}$ was modified to contain an N-terminal SpyCatcher[34] and a C-terminal AviTag (Avidity). The protein was purified by Ni-NTA affinity and incubated overnight with 0.03% H_2O_2 to induce disulfide formation. Buffer was exchanged via dialysis for the biotinylation reaction, followed by gel filtration as described previously[35]. The octamer protein was finally reacted with a HaloTag-SpyTag construct, purified via Ni-NTA affinity and gel filtration. **Single molecule recordings:** A solution containing ~10 nM $I27^{OXD}$ was added to the flow cell for 20 minutes and was washed out with an experimental buffer consisting of PBS buffer pH 7.4 containing 10 mM ascorbate to prevent nonspecific oxidation of cysteine thiols and other side chains[36]. Streptavidin beads blocked were blocked the previous night with 1% BSA in PBS, which was exchanged to the experimental PBS/ascorbate buffer immediately before the experiment. 50 uL of the streptavidin beads were flowed through the chamber and allowed to settle on the bottom coverslip, after which the permanent magnets were brought down to a resting position that applies 4 pN to the beads. Fresh experimental buffer was frequently exchanged into the flow cell, every ~30 minutes, due to evaporative losses from the open ends of the flow cell.

Author Contributions

The experiments were designed by ECE, JARP, and JMF. Experimental data was collected by ECE, SH, and JARP. Data processing and analysis was done by ECE, SH, and RTR. Writing of the manuscript was done by ECE and JMF.

References

1. Ilton, M. *et al.* The principles of cascading power limits in small, fast biological and engineered systems. *Science* **360,** eaao1082 (2018).
2. Mahadevan, L. & Matsudaira, P. Motility Powered by Supramolecular Springs and Ratchets. *Science* **288,** 95–99 (2000).
3. Li, H. *et al.* Reverse engineering of the giant muscle protein titin. *Nature* **418,** 998 (2002).
4. Lee, G. *et al.* Nanospring behaviour of ankyrin repeats. *Nature* **440,** 246–249 (2006).
5. Rief, M., Pascual, J., Saraste, M. & Gaub, H. E. Single molecule force spectroscopy of spectrin repeats: low unfolding forces in helix bundles11Edited by W. Baumeister. *J. Mol. Biol.* **286,** 553–561 (1999).
6. Manteca, A. *et al.* Mechanochemical evolution of the giant muscle protein titin as inferred from resurrected proteins. *Nat. Struct. Mol. Biol.* **24,** 652–657 (2017).
7. Giganti, D., Yan, K., Badilla, C. L., Fernandez, J. M. & Alegre-Cebollada, J. Disulfide isomerization reactions in titin immunoglobulin domains enable a mode of protein elasticity. *Nat. Commun.* **9,** 185 (2018).
8. Wiita, A. P., Ainavarapu, S. R. K., Huang, H. H. & Fernandez, J. M. Force-dependent chemical kinetics of disulfide bond reduction observed with single-molecule techniques. *Proc. Natl. Acad. Sci.* **103,** 7222–7227 (2006).
9. Rivas-Pardo, J. A. *et al.* Work Done by Titin Protein Folding Assists Muscle Contraction. *Cell Rep.* **14,** 1339–1347 (2016).
10. Popa, I. *et al.* A HaloTag Anchored Ruler for Week-Long Studies of Protein Dynamics. *J. Am. Chem. Soc.* **138,** 10546–10553 (2016).
11. Howard, J. Molecular motors: structural adaptations to cellular functions. *Nature* **389,** 561–567 (1997).
12. Svoboda, K. & Block, S. M. Force and velocity measured for single kinesin molecules. *Cell* **77,** 773–784 (1994).
13. Finer, J. T., Simmons, R. M. & Spudich, J. A. Single myosin molecule mechanics: piconewton forces and nanometre steps. *Nature* **368,** 113–119 (1994).
14. Sun, S., Footer, M. & Matsudaira, P. Modification of Cys-837 identifies an actin-binding site in the beta-propeller protein scruin. *Mol. Biol. Cell* **8,** 421–430 (1997).
15. Way, M., Sanders, M., Garcia, C., Sakai, J. & Matsudaira, P. Sequence and domain organization of scruin, an actin-cross-linking protein in the acrosomal process of Limulus sperm. *J. Cell Biol.* **128,** 51–60 (1995).
16. Theriot, J. A., Mitchison, T. J., Tilney, L. G. & Portnoy, D. A. The rate of actin-based motility of intracellular Listeria monocytogenes equals the rate of actin polymerization. *Nature* **357,** 257–260 (1992).
17. Forscher, P., Lin, C. H. & Thompson, C. Novel form of growth cone motility involving site-directed actin filament assembly. *Nature* **357,** 515–518 (1992).
18. Merz, A. J., So, M. & Sheetz, M. P. Pilus retraction powers bacterial twitching motility. *Nature* **407,** 98–102 (2000).
19. Fernandez, J. M. & Li, H. Force-Clamp Spectroscopy Monitors the Folding Trajectory of a Single Protein. *Science* **303,** 1674–1678 (2004).
20. Eckels, E. C., Tapia-Rojo, R., Rivas-Pardo, J. A. & Fernández, J. M. The Work of Titin Protein Folding as a Major Driver in Muscle Contraction. *Annu. Rev. Physiol.* **80,** null (2018).
21. Flory, P. J. *Principles of Polymer Chemistry*. (Cornell University Press, 1953).
22. Ainavarapu, S. R. K. *et al.* Contour Length and Refolding Rate of a Small Protein Controlled by Engineered Disulfide Bonds. *Biophys. J.* **92,** 225–233 (2007).
23. Huxley, A. F. & Simmons, R. M. Proposed Mechanism of Force Generation in Striated Muscle. *Nature* **233,** 533–538 (1971).

24. Chen, H. *et al.* Dynamics of Equilibrium Folding and Unfolding Transitions of Titin Immunoglobulin Domain under Constant Forces. *J. Am. Chem. Soc.* **137,** 3540–3546 (2015).
25. Dudko, O. K., Hummer, G. & Szabo, A. Theory, analysis, and interpretation of single-molecule force spectroscopy experiments. *Proc. Natl. Acad. Sci.* **105,** 15755–15760 (2008).
26. Piazzesi, G. *et al.* Skeletal Muscle Performance Determined by Modulation of Number of Myosin Motors Rather Than Motor Force or Stroke Size. *Cell* **131,** 784–795 (2007).
27. Caremani, M. *et al.* Size and speed of the working stroke of cardiac myosin in situ. *Proc. Natl. Acad. Sci.* **113,** 3675–3680 (2016).
28. Linari, M. *et al.* Force generation by skeletal muscle is controlled by mechanosensing in myosin filaments. *Nature* **528,** 276–279 (2015).
29. Feng, W., Liu, G., Allen, P. D. & Pessah, I. N. Transmembrane Redox Sensor of Ryanodine Receptor Complex. *J. Biol. Chem.* **275,** 35902–35907 (2000).
30. Oba, T., Murayama, T. & Ogawa, Y. Redox states of type 1 ryanodine receptor alter Ca2+ release channel response to modulators. *Am. J. Physiol.-Cell Physiol.* **282,** C684–C692 (2002).
31. Xia, R., Stangler, T. & Abramson, J. J. Skeletal Muscle Ryanodine Receptor Is a Redox Sensor with a Well Defined Redox Potential That Is Sensitive to Channel Modulators. *J. Biol. Chem.* **275,** 36556–36561 (2000).
32. Beckendorf, L. & Linke, W. A. Emerging importance of oxidative stress in regulating striated muscle elasticity. *J. Muscle Res. Cell Motil.* **36,** 25–36 (2015).
33. Debold, E. P., Patlak, J. B. & Warshaw, D. M. Slip Sliding Away: Load-Dependence of Velocity Generated by Skeletal Muscle Myosin Molecules in the Laser Trap. *Biophys. J.* **89,** L34–L36 (2005).
34. Zakeri, B. *et al.* Peptide tag forming a rapid covalent bond to a protein, through engineering a bacterial adhesin. *Proc. Natl. Acad. Sci.* **109,** E690–E697 (2012).
35. Kosuri, P. *et al.* Protein Folding Drives Disulfide Formation. *Cell* **151,** 794–806 (2012).
36. Valle-Orero, J. *et al.* Mechanical Deformation Accelerates Protein Ageing. *Angew. Chem. Int. Ed.* **56,** 9741–9746 (2017).

Figures

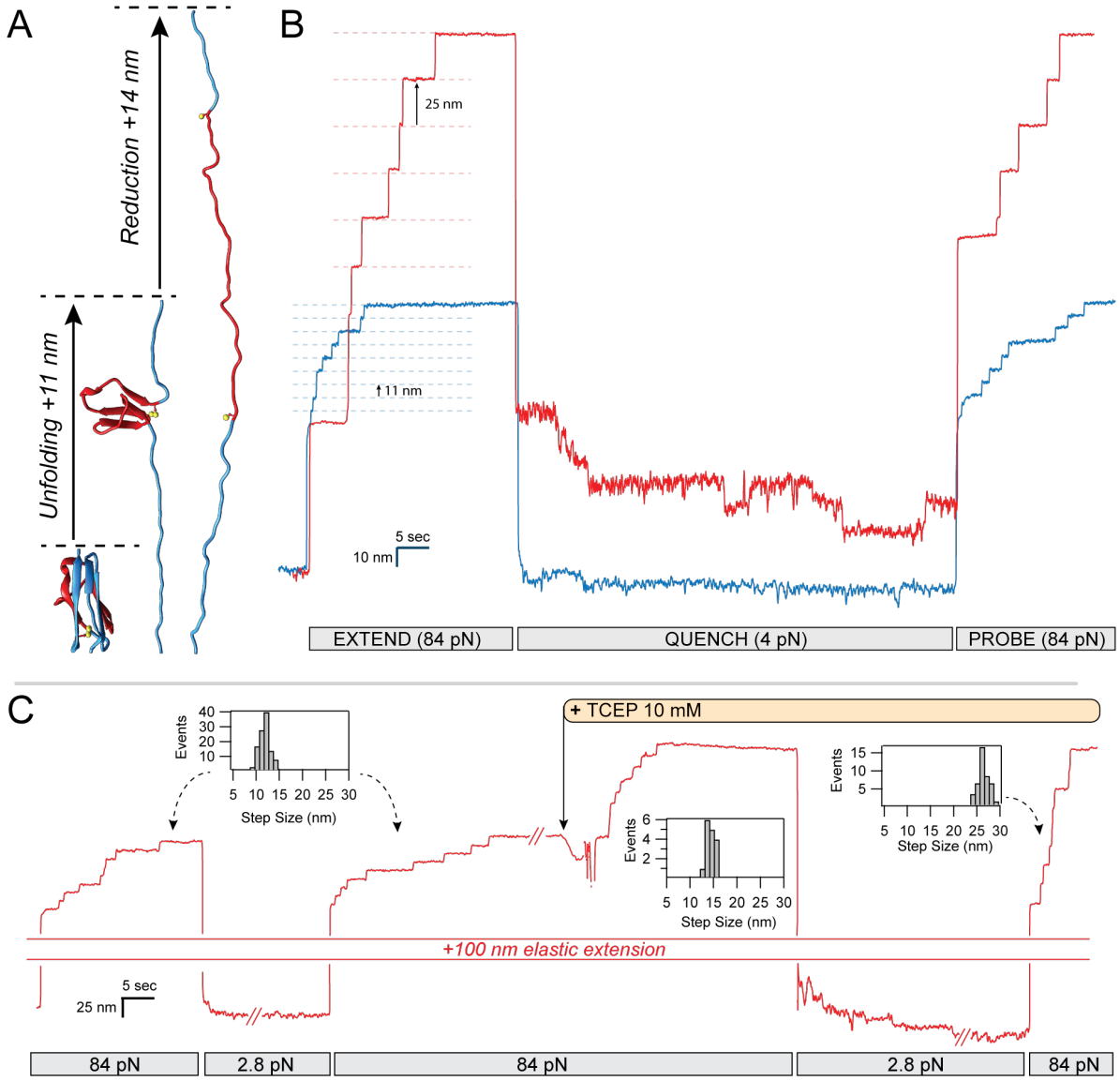

Figure 1: Real-time control of cryptic disulfide bonds in single polyproteins under force. (A) Under force, an Ig domain extends up to its buried disulfide bond, exposing it. Upon reduction, a further extension occurs. **(B)** The oxidation status and effect of cryptic disulfide bonds are evident in these two traces of polyproteins containing eight repeats of a titin Ig domain. Oxidized polyproteins extending at a high force of 84 pN increase their length in steps of 11 nm (blue trace), whereas reduced polyproteins extend in steps of 25 nm (red trace). While the rate of folding of the reduced polyprotein at 4 pN is slow, oxidation greatly accelerates the folding rate, driving it to completion at the same force. The increased folding probability at 4 pN is measured from the number of steps recovered with a probe pulse at 84 pN (red trace 4, blue trace 8). **(C)** The status of a single polyprotein can be easily changed from oxidized to reduced by introducing a reducing agent into the solution (TCEP), while the polyprotein is fully unfolded, exposing its thiols to the solution. Step size histograms record the changes observed from extending a fully oxidized polyprotein (11.4 +/- 2.1 nm); immediately after addition of TCEP (14.6 +/- 1.6 nm) and after refolding the resulting fully reduced polyprotein (25.6 +/- 2.2 nm).

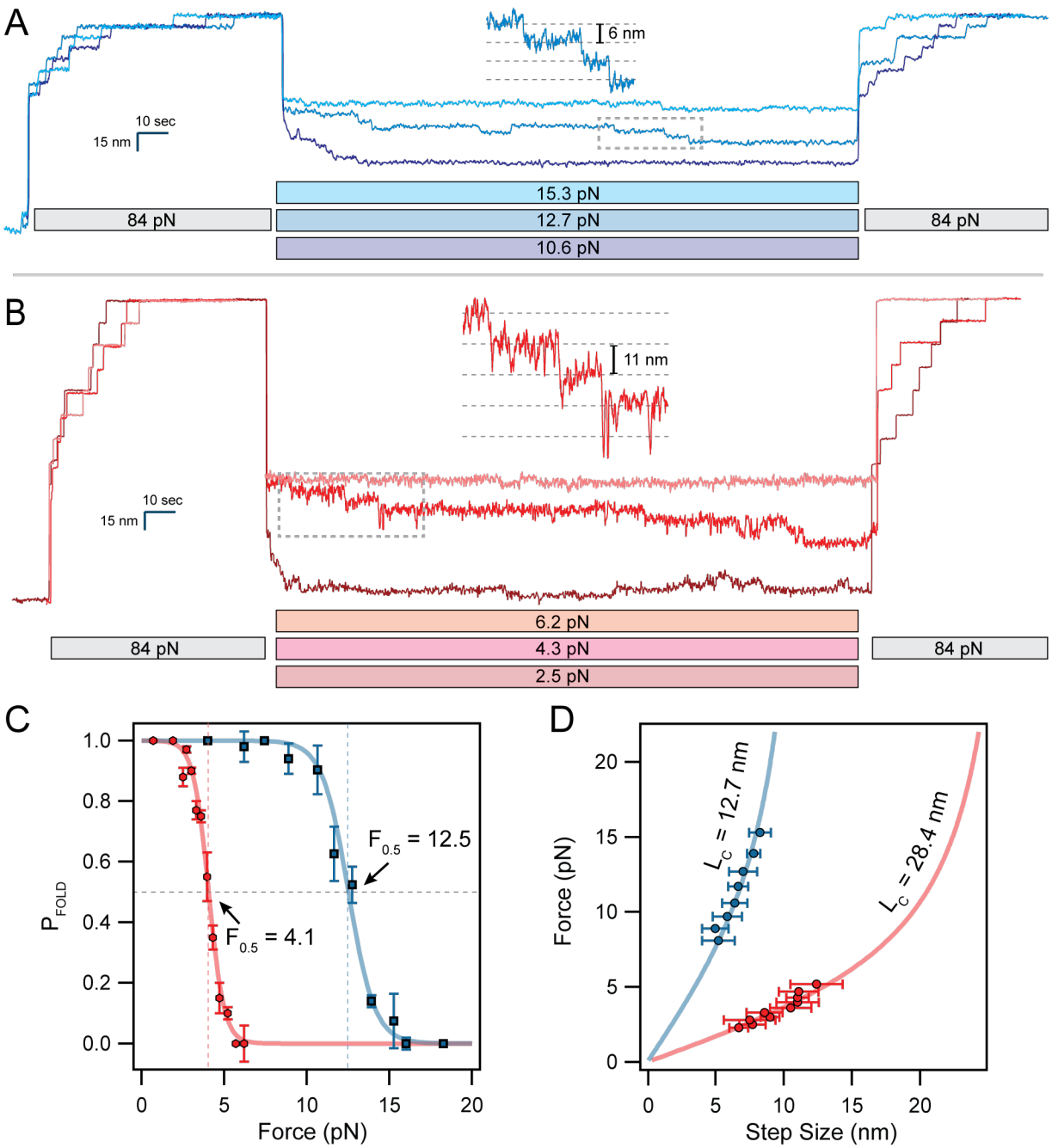

Figure 2: Cryptic disulfide bonds alter the folding dynamics of titin Ig domains. (A) After full extension, oxidized polyproteins are allowed to fold by quenching the force to 10-16 pN for 100 sec. While only a single folding event is observed at 16 pN, complete refolding occurs at 10.6 pN. **(B)** Reduced polyproteins fold at a much lower range of forces in the 2-5 pN range. **(C)** The folding probability is calculated as the number of refolded domains (probe pulse) divided by eight. Oxidation shifts the midpoint folding probability from 4.1 pN to 12.5 pN. The data was collected from several different molecules, with n=11 for $I27^{OXD}$ and n=9 for $I27^{RED}$ **(D)** The folding steps observed during the quench pulse (insets in A and B) scale in size with the applied force. Oxidized folding steps (blue circles) are fit by the FJC model (solid blue line, see supplementary equations) using a contour length of 12.7 nm. Reduced folding steps (red circles) are fit using a much larger contour length of 28.4 nm (solid red line). These data came from the same molecules measured in panel (C).

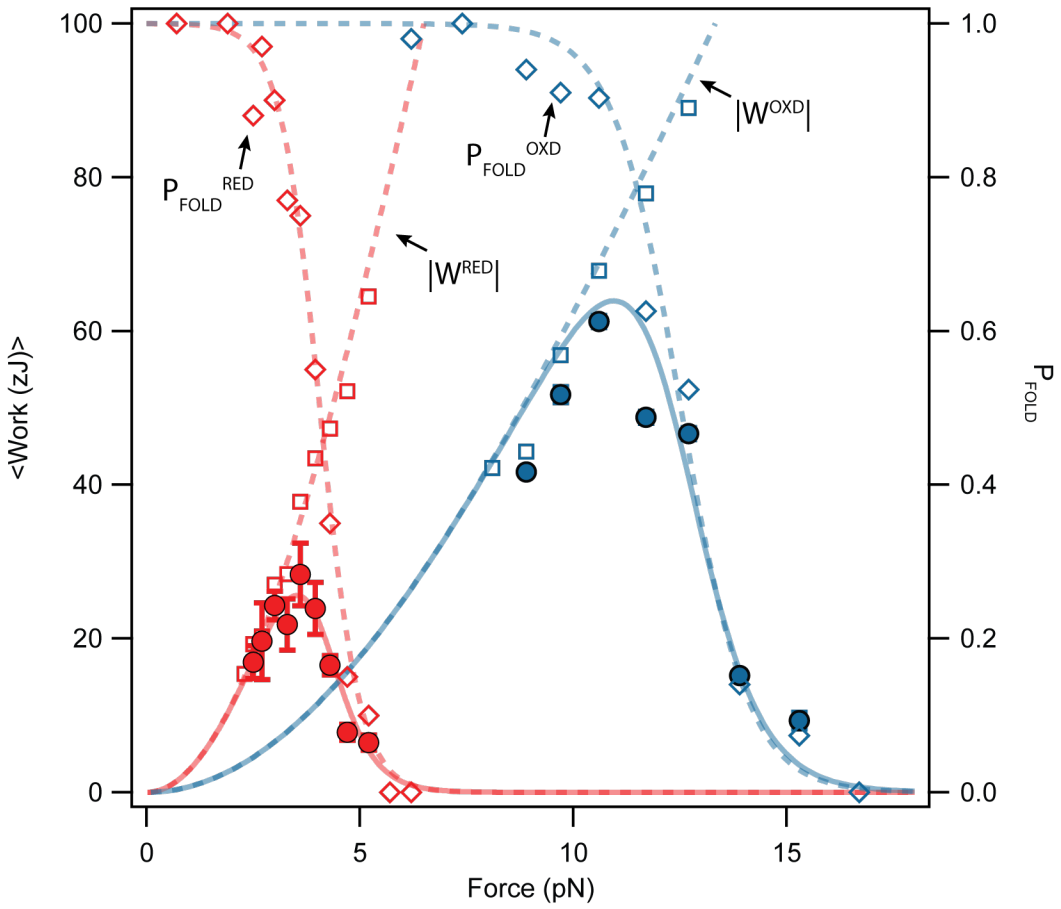

Figure 3: Oxidation increases the work done by protein folding and shifts its peak to higher forces. We calculate the expected value of the work delivered by folding steps as the product of folding work times the folding probability. The expected value of the folding work delivered by a reduced Ig domain peaks at force of 3.5 pN with a value of 25.6 zJ (solid red line), calculated by multiplying the reduced folding probability (empty red squares, dashed line) times the reduced folding work (empty red diamonds, dashed line). Oxidation causes large effects on the mechanical work delivered by protein folding: the expected value of the folding work delivered by an oxidized Ig domain is now 2.5 times bigger (63.9 zJ) and peaks at 11 pN (solid blue line; from the oxidized folding probability (empty blue diamonds, dashed line) times the oxidized folding work (empty blue squares, dashed line). However, in both cases, the delivery of the folding work at their peak is very slow due to measured folding kinetics.

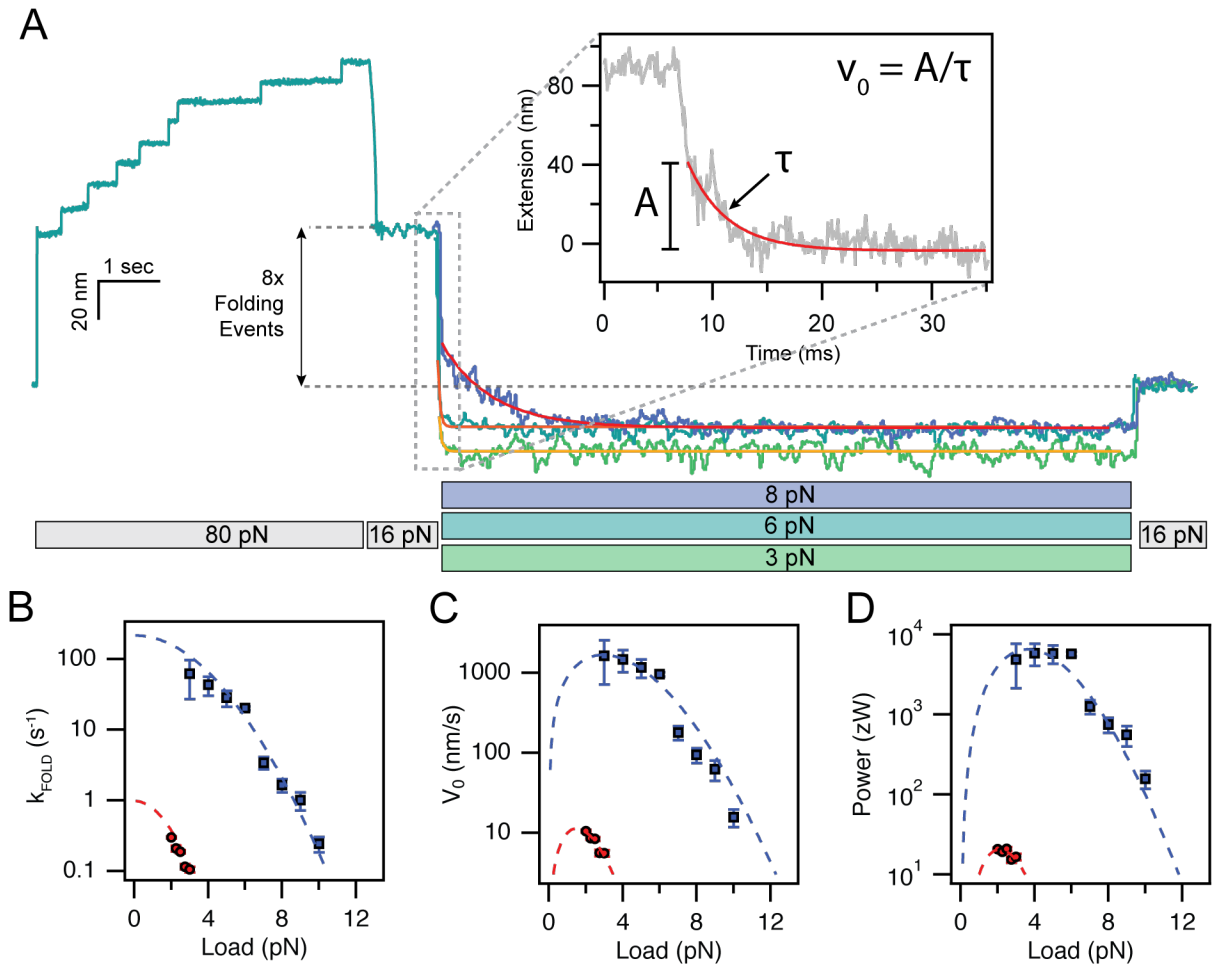

Figure 4: Oxidation acts as a power switch controlling the delivery of protein folding work. (A) Force protocol for measuring fast folding contractions at forces where the folding probability is always one. A fully extended oxidized polyprotein is first quenched to 16 pN, where no folding occurs. A rapid quench follows, resulting into a brief elastic recoil and a very fast folding contraction. A subsequent increase of the force up to 16 pN reveals a much shorter extension, marking the folding of all eight domains. The speed of the folding contraction increases greatly as the force of the quench is reduced. The folding contractions are fit with a single exponential to measure the folding rate. **(B)** Shows the force dependency of the folding rate for oxidized domains (blue squares) and reduced domains (red squares). The dashed lines correspond to fits using equation 1. **(C)** Force dependency of the initial velocity of the folding contraction (V_0), measured as the amplitude of the contraction divided by its time constant (inset, panel A). The dashed lines correspond to fits from fits from equation 2. **(D)** the power delivered by the folding contraction is then calculated as $V_0 \cdot F$. The dashed lines are fits of equation 3. The figure shows that oxidation of the polyprotein increases the peak output power of its folding contraction by more than 300 fold, reaching ~ 6600 zW. Data was averaged from n=5 molecules for $I27^{OXD}$ and from n=3 molecules for $I27^{RED}$.